



resistance, and should be controlled by tempering parameters, allowing for the specific loading conditions.

3. The efficiency is shown of improving wear resistance by combining hardfacing with the low-carbon Cr–Mn-based metal and subsequent case hardening.

1. Ryabtsev, I.A. (2004) *Hardfacing of machine parts and mechanisms*. Kiev: Ekotekhnologiya.
2. Malinov, L.S., Chejlyakh, A.P. (1981) Chrome-manganese steels of transition grade. *Izvestiya Vuzov. Chyorn. Metallurgiya*, **4**, 101–103.
3. Malinov, L.S., Chejlyakh, A.P. (1983) Effect of manganese and heat treatment on structure and properties of steels Fe–0,1 % C–14 % Cr. *Ibid.*, **6**, 83–87.
4. Malinov, L.S., Malinov, V.L. (2009) *Resource-saving sparsely alloyed alloys and hardening technologies providing the effect of self-hardening*. Mariupol: Renata.
5. Malinov, V.L. (2011) Effect of manganese on structure and wear resistance of deposited metal of the low-carbon steel type. *The Paton Welding J.*, **8**, 12–16.
6. Tylkin, M.A. (1965) *Strength and wear resistance of metallurgical equipment parts*. Moscow: Metallurgiya.
7. Popov, V.S., Brykov, I.N. (1996) *Wear resistance of steels and alloys*. Zaporozhie: IPK Zaporozhie.
8. Malinov, L.S., Konop-Lyashko, V.I. (1982) Effect of ageing on development of martensitic transformation in deformation of meta-stable austenitic steels. *Izvestiya AN SSSR. Metall.*, **3**, 130–133.
9. Gladky, P.V., Kondratiev, I.A., Yumatova, V.I. et al. (1991) *Hardfacing flux-cored strips and wires*: Refer. Book. Kiev: Tekhnika.
10. Malinov, V.L. *Charge of flux-cored strip*. Pat. 94862 Ukraine. Int. Cl. C2 B23K 35/28. Fil. 07.06.2010. Publ. 11.06.2011.
11. Malinov, L.S., Malinov, V.L. *Method of hardening*. Pat. 63462 Ukraine. Int. Cl. C 21 D1/2. Fil. 22.04.2003. Publ. 15.01.2004.
12. Pikalov, S.V. (2009) About possibilities of repair of automobile parts by gas-shielded surfacing with subsequent case hardening. In: *Proc. of 1st Int. Sci.-Techn. Conf. on Current Automobile Materials and Technologies*, 216–223. Kursk: STU.
13. Malinov, L.S., Chejlyakh, A.P., Malinova, E.L. (1991) Effect of case hardening and subsequent heat treatment on structure, phase composition and abrasive wear resistance of Fe–Cr–Mn steels. *Izvestiya AN SSSR. Metall.*, **1**, 120–123.

PECULIARITIES OF STRUCTURE AND MECHANICAL HETEROGENEITY IN EB-WELDED JOINTS OF 1201-T ALLOY

V.R. SKALSKY¹, L.R. BOTVINA² and I.N. LYASOTA¹

¹H.V. Karpenko Physico-Mechanical Institute, NASU, Lvov, Ukraine

²A.A. Baikov Institute of Metallurgy and Materials Science, RAS, Moscow, Russia

The peculiarities of microstructure and distribution of microhardness of weld and heat-affected zone metal of welded joints of 1201-T alloy, produced using electron beam welding at different values of heat input, were studied. Using plotted temperature fields the running of phase transformations occurred in welding was analyzed. It was established that due to change of cooling rate across the thickness of plates the microstructure of near-weld zone in upper and lower parts of welded joint were considerably different. The increase of heat input of welding facilitates recrystallization processes which leads to increase of heat-affected zone.

Keywords: *electron beam welding, aluminium alloy, heat-affected zone, weakening, temperature field, structure and mechanical heterogeneity, microstructure*

Due to high strength and resistance to cryogenic and corrosion embrittlement the aluminium alloys of Al–Cu–Mn system are widely applied in aircraft industry [1, 2]. For joining critical elements of structures the electron beam welding (EBW) is applied as far as this method provides high quality of weld metal in one-pass welding large thicknesses [3]. The characteristic property of thermal cycle of welding is rapid heating of metal and also its cooling. The short periods of this process provide special kinetics of structural transformations which results in weakening and heterogeneity of welded joints (WJ) [4–12]. It is the most clearly revealed in welding of thick plates and caused by decay of solid solution of copper in aluminium and partial coagulation of strengthening phases due to uniform heating of weld and adjacent zones of base metal [4].

Elements of structures of aluminium alloys containing WJ are operating under conditions of alter-

nating dynamic loads, deep vacuum and cryogenic temperatures, which frequently results in initiation and propagation of micro- and macrofracture in them. The process of microcrack propagation depends directly on the structure and mechanical characteristics of metal. Therefore, to perform efficient diagnostics of WJ of structure elements manufactured of mentioned aluminium alloy including methods of acoustic emission [5–7], it is important also to investigate the microstructure of HAZ metal.

The purpose of the work is to study peculiarities of structure and mechanical heterogeneity of WJ of thick plates of heat-hardened 1201-T alloy, produced using EBW.

It is known that level of weakening and structure changes in HAZ metal of WJ of heat-hardened aluminium alloys is determined by welding cycle and structure of base metal [8–10]. It was also established [11] that a weld is weakened to the level characteristic for metal in annealed state (for 1201 alloy to *HRB* 70). This phenomenon is predetermined by both the processes of dissolution of strengthening phases as well as their further precipitation during cooling.

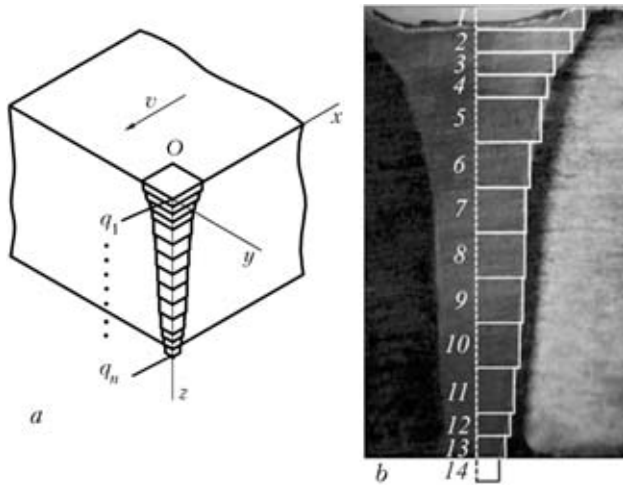


Figure 1. Scheme of modeling of splitting moving linear power sources across the thickness of plates (a), and macrosection of WJ of 1201-T alloy (b)

In works [9, 11, 12] the influence of welding method on the width of weakening zone of WJ of aluminium alloys was studied. It was shown that this area is narrower in EBW as compared to that of argon arc welding, thus influencing mechanical properties of these WJ and general strength of the structure [13]. To increase properties of WJ they are subjected to heat treatment, which for dispersion-strengthened alloys (including 1201 alloy) consists in tempering and further artificial ageing [14]. The influence of post-weld heat treatment on the structure and mechanical characteristics of WJ were investigated in works [9–11, 14–17]. It was established that such heat treatment allows increasing hardness of 1021 alloy weld metal only by 10 %. Thus, the repeated artificial ageing practically does not change the strength characteristics of these WJ.

The investigations of structural transformations in HAZ metal of 2219 alloy showed that the zone of high temperature dissolution of strengthening phases is formed independently of initial structure of base metal

[18]. It is explained by the fact that heating of HAZ metal in vicinity of fusion boundary exceeds the temperature of hardening. Under these conditions the dissolution of precipitates occurs, and the further rapid cooling facilitates the formation of main strengthening particles. The low-temperature dissolution of strengthening phases, except of thermal cycle of welding, depends on initial structure of base metal. Its level at low temperatures (523–573 K) is determined by the size of precipitates, type of crystalline lattice and coherency relatively to the matrix. The dissolution of coherent particles occurs more intensively than non-coherent ones, i.e. Guinier–Preston zones are dissolved more rapidly than θ -phase. Between the areas of high- and low-temperature dissolution of strengtheners more equilibrium phases can be formed accompanying by annealing of alloy.

To investigate WJ of 20 and 25 mm thickness produced using through EBW without filler metal the following conditions were used: welding speed $v_w = 70$ m/h; beam current $I_b = 120$ (180) A; acceleration voltage $U_{acc} = 60$ (55) kV; heat input $q/v = 337.3$ (463.7) kJ/m. The plates to be welded were manufactured of heat-hardened aluminium 1201-T alloy.

It is known [11] that dynamics of structural transformations in each point of HAZ depends on maximum temperature of their heating and time of remaining in the corresponding temperature range. Therefore for better analysis of metallurgy processes running in EBW of thick plates of aluminium alloys, it is necessary to calculate the temperature field and thermal cycles in HAZ metal of WJ.

To plot temperature fields the methods were applied described in [19]. Its principle consisted in fact that in EBW the channel of penetration is considered as totality of linear heat sources q_i ($i = 1, \dots, n$) of general power q , moving at the speed of welding in the middle of plates (Figure 1, a). Therefore, the sum of temperature fields of separate linear sources deter-

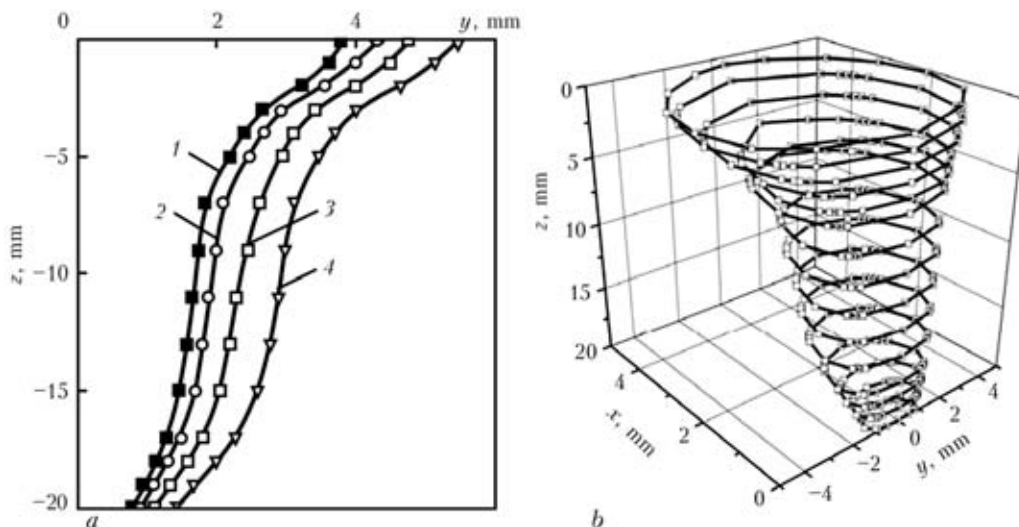


Figure 2. Isotherms in the plane yOz (a) (1 – 853; 2 – 773; 3 – 673; 4 – 573 K), and isothermic surface at $T = 673$ K (b) in EBW of plates 20 mm thick

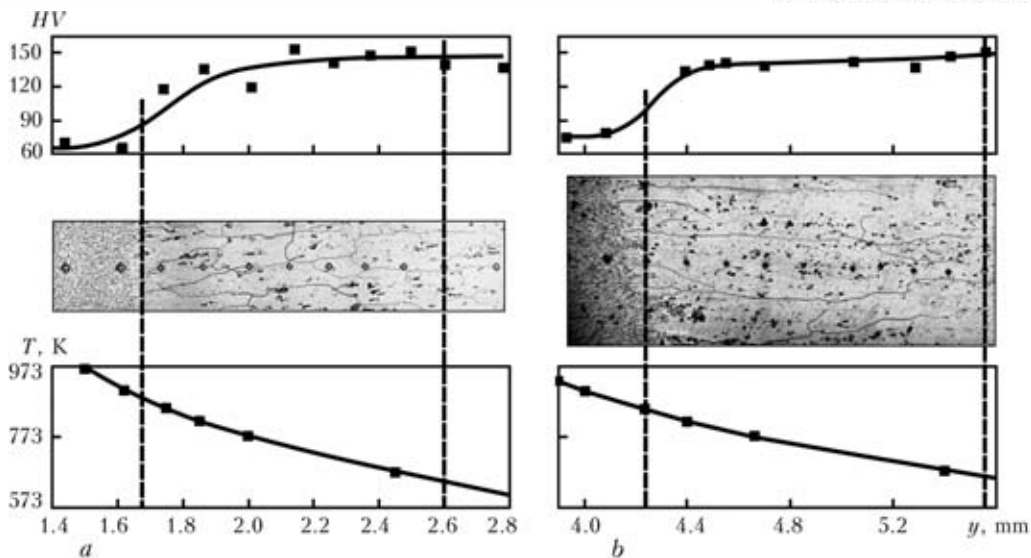


Figure 3. Distribution of microhardness and microstructure of HAZ metal of WJ at $q/v = 337.3$ (a) and 463.7 (b) kJ/m at removing from the weld axis

mines the general field. Such optimal amount of power sources is offered to provide minimal thickness of splitting layer within the range of 1–5 mm. The distribution of temperatures from such a source was determined according to the model of N.N. Rykalin [20]. For accurate calculation of geometry of a fusion boundary in the areas, where considerable nonlinearity of its form is observed, this area was split into more finer layers (Figure 1, b). The advantage of this method in welding of thick-wall structure elements is consideration of uniformity of distribution of energy of heat source across the section of a joint.

The hardness of WJ metal was measured using microhardness meter PMT-3. The loading on indenter was 0.54 Pa.

The results of calculations presented in Figure 2 show that fields are non-uniform according to all three spatial coordinates, which, in its turn, is the reason of non-uniform heating of HAZ points along the WJ section. The characteristic concentricity of isothermal field (Figure 2, b) is predetermined by physical properties of aluminium alloys, in particular, their high heat conductivity, significantly influencing the processes of heat distribution in welding [21].

Figure 3 shows that changes in HAZ metal occur already at the temperature of 723 K. The clear etching of structure components is observed caused by partial coagulation of strengthening phases which precipitated in the bulk of grains and along their boundaries.

The characteristic peculiarities of thermal influence in EBW is rapid heating of metal up to maximum temperatures and slower rate of its further cooling (Figure 4). In welding of artificially aged alloy in the period of its rapid heating the coagulation processes do not manage to run over, and during further cooling starting from the temperature of 823 K and lower high-temperature decay of solid solution occurs which is followed by formation of strengthener. The originates of θ -phase are, first of all, formed along the

grain boundaries [4], as far as these areas contain impurities of different type, and also in the body of a grain. Their development occurs due to coming of atoms of copper from the surrounding solution. Thus, the grain boundaries are getting thicker at their removing from base metal to fusion line and light near-boundary areas of aluminium solution, depleted with copper, arise, that, in its turn, facilitates decrease in metal hardness.

Depending on the time of remaining of metal in the temperature range of 573–823 K the conditions for complete decay of solid solution, coagulation of precipitated phase Al_2Cu and recrystallization processes are formed. Figure 4 shows thermal cycles of spots located in different zones of WJ. Due to decrease of q/v across the thickness of WJ the instant rate of cooling is increased from the beginning of counting out to the direction of z axis. It is evidenced by the changes of inclination of curves 1–3 in Figure 4 at the stage of cooling. In connection with different time of remaining in temperature range mentioned above the level of recrystallization and precipitation of strengthening phase is differed. The analysis of microstructure (Figure 5) shows that grains of HAZ metal of upper

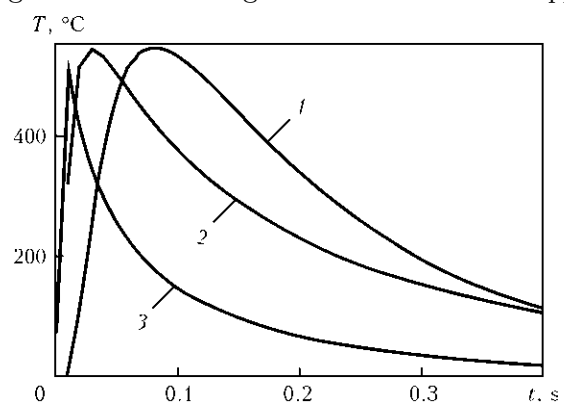


Figure 4. Thermal cycles of points located in different zones of WJ: 1 – $y = 3.76$ mm, $z = 0$; 2 – $y = 1.84$ mm, $z = 10$ mm; 3 – $y = 0.83$ mm, $z = 20$ mm

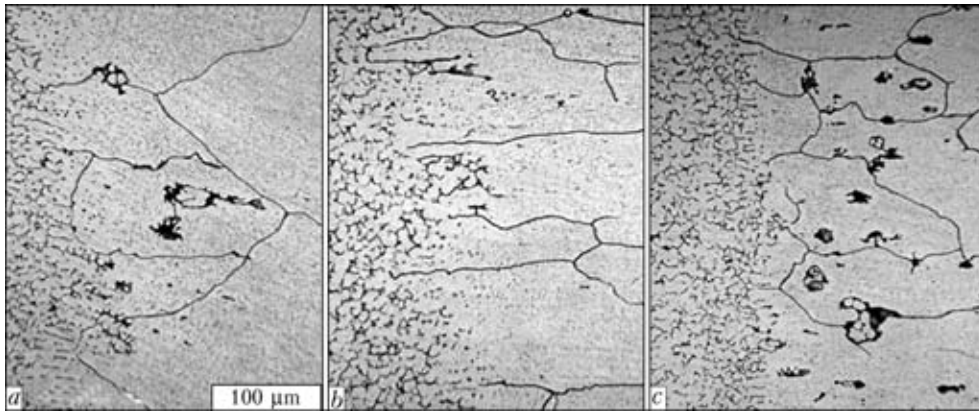


Figure 5. Microstructures of upper (*a*), central (*b* – $\times 150$) and lower (*c* – $\times 150$) areas of fusion zone of aluminium 1201-T alloy WJ at $q/v = 337.3$ kJ/m

part of WJ (Figure 5, *a*) are considerably larger than those of central and lower one (Figure 5, *b* and *c*, correspondingly). The grains of upper part of fusion boundary are also strengthened by fine precipitates of Al_2Cu phase, however in a lower one they are depleted as far as θ -phase are mainly distributed along their boundaries. The increase of heat input of welding facilitates intensifying of these processes which correspondingly leads to increase of HAZ (see Figure 3).

Thus, the course of dissolution and repeated formation of solid solution, its decay and coagulation of separate particles form mechanical characteristics of near-weld zone. The fusion of grains at the fusion boundary and formation of constant brittle eutectic interlayers along their boundaries facilitate embrittlement of alloy, and recrystallization and growth of grains decrease strength and crack resistance of WJ [11, 22, 23]. Therefore, it is important to consider these phenomena during diagnostics and investigation of processes of initiation of fracture of structures containing such WJ.

It should be noted in conclusion that investigation of microstructure and hardness of WJ of heat-hardened aluminium 1201-T alloy, produced using EBW, showed that the given material tends to considerable decay of solid solution and weakening of weld and HAZ metal. As a result of changes in cooling rate across the thickness of plates, the microstructure of near-weld zone of upper and lower part of WJ is different. The increase of heat input of welding facilitates the processes of recrystallization and leads to increase of sizes of HAZ: at $q/v = 337.3$ kJ/m the width of this area is 0.9 mm, and at $q/v = 463.7$ kJ it is of 1.4 mm, the extension of grains reaches on average 0.5–0.9 mm. As a result all these phenomena can negatively influence the mechanical properties of these joints.

1. Ishchenko, A.Ya. (2004) Specifics in application of aluminium high-strength alloys for welded structures. *The Paton Welding J.*, **9**, 15–25.
2. Ishchenko, A.Ya. (2007) Welding of aluminium alloys (directions of research conducted at PWI). *Ibid.*, **11**, 6–9.

3. Paton, B.E., Bondarev, A.A. (2004) State-of-the-art and advanced technologies of electron beam welding of structures. *Ibid.*, **11**, 20–27.
4. Nikiforov, G.D. (1972) *Metallurgy of fusion welding of aluminium alloys*. Moscow: Mashinostroenie.
5. Skalsky, V.R., Sergienko, O.M., Golaski, L. (1999) Generation of acoustic emission by cracks propagated in welded joints. *Tekhn. Diagnostika i Nerazrush. Kontrol*, **4**, 23–31.
6. Skalsky, V.R., Andrejkiv, O.E. (2006) *Assessment of volume damage of materials by acoustic emission method*. Lviv: I. Franko Lviv NU.
7. Skalsky, V.R. (2001) Procedure of assessment of defect formation in alloys D16-T and 1201-T by acoustic emission method. *Mashynoznavstvo*, **3**, 13–18.
8. Rabkin, D.M. (1986) *Metallurgy of fusion welding of aluminium and its alloys*. Kiev: Naukova Dumka.
9. Rabkin, D.M., Lozovskaya, A.V., Sklabinskaya, I.E. (1992) *Metals science of aluminium and its alloys*. Kiev: Naukova Dumka.
10. Ishchenko, A.Ya., Lozovskaya, A.V. (1980) Kinetics of transformations in welding of heat-hardened aluminium alloy 1201. *Avtomatich. Svarka*, **1**, 29–32.
11. Lozovskaya, A.V., Chajka, A.A., Bondarev, A.A. et al. (2001) Softening of high-strength aluminium alloys in different fusion welding processes. *The Paton Welding J.*, **3**, 13–17.
12. Bondarev, A.A., Lozovskaya, A.V., Ishchenko, A.Ya. et al. (1974) Specifics of electron beam welding of alloy 1201. *Avtomatich. Svarka*, **2**, 20–22.
13. Malarvizhi, S., Alasubramanian, V. (2011) Effect of welding processes on AA2219 aluminium alloy joint properties. *Transact. of Nonferrous Metals Soc. of China*, **21(5)**, 962–973.
14. Frolov, V.V. (2003) *Arc welding of aluminium*. Kharkov: Tekhnologiya.
15. Malarvizhi, S., Alasubramanian, V. (2010) Effects of welding processes and post-weld aging treatment on fatigue behavior of AA2219 aluminium alloy joints. *J. Mat. Eng. and Performance*, **20(3)**, 359–367.
16. Tosto, S., Nenci, F., Hu, J. (1996) Microstructure and properties of electron beam welded and post-welded 2219 aluminium alloy. *Mat. Sci. and Technol.*, **12**, 323–328.
17. Alapati, R., Dwivedi, D.K. (2009) Microstructure and hardness of Al–Cu alloy (A2218) welded joints produced by GTAW. *The Paton Welding J.*, **4**, 21–26.
18. Ishchenko, A.Ya., Lozovskaya, A.V., Sklabinskaya, I.E. (2001) Physical simulation of heat processes in HAZ metal during welding aluminium-lithium alloys. *Ibid.*, **9**, 4–7.
19. Skalsky, V.R., Lyasota, I.M. (2010) Estimation of the heat-affected zone for the electron-beam welding of plates. *Mat. Sci.*, **46(1)**, 115–123.
20. Rykalin, N.N. (1951) *Calculations of thermal processes in welding*. Moscow: Mashinostroenie.
21. Dilthey, U. (2005) *Schweisstechnische Fertigungsverfahren 2. Verhalten der Werkstoffe beim Schweißen*. Vol. XXII. Springer.
22. Bondarev, A.A., Golikov, V.N., Anisimov, Yu.I. (1987) Resistance to brittle fracture of electron beam welded joints of aluminium alloy 1201. *Avtomatich. Svarka*, **3**, 6–7.
23. Labur, T.M., Ishchenko, A.Ya., Taranova, T.G. (1991) Resistance to fracture of welded joints of high-strength aluminium alloys 1151 and 1201. *Ibid.*, **6**, 39–41.